

NEW RADIO AND OPTICAL STUDY OF THE SUPERNOVA REMNANT W44

E. B. GIACANI,¹ AND G. M. DUBNER¹

Instituto de Astronomía y Física del Espacio (CONICET, UBA) C.C.67, 1428 Buenos Aires, Argentina
 Electronic mail: egiacani@iafe.uba.ar; gdubner@iafe.uba.ar

N. E. KASSIM

Remote Sensing Division, Naval Research Laboratory, Washington D. C. 220375-5000
 Electronic mail: nkassim@shimmer.nrl.navy.mil

D. A. FRAIL AND W. M. GOSS

National Radio Astronomy Observatory, Very Large Array, P.O. Box 0, Socorro, New Mexico 87801
 Electronic mail: dfrail@nrao.edu; mgoss@nrao.edu

P. F. WINKLER² AND B. F. WILLIAMS²

Department of Physics, Middlebury College, Middlebury, Vermont 05753
 Electronic mail: winkler@midd.cc.middlebury.edu

Received 1996 July 22; revised 1996 December 18

ABSTRACT

We present new optical images of the supernova remnant (SNR) W44 in the $H\alpha$ and $[S\ II]$ lines covering the entire source for the first time. We also report on improved radio image of W44 at 1442.5 MHz, obtained after the reprocessing of existing VLA data. A spectral index α of -0.4 was derived for the whole source, without indication of significant spectral variations between 0.3 and 1.4 GHz across the remnant. Accurate multiwavelength comparisons were made based on existing observations of W44 in the different spectral regimes. We find excellent correlation between optical and radio emission along the northwest border of the remnant, suggesting that the optical radiation is originating through radiative cooling of the shocked gas immediately behind the shock front. Some diffuse optical emission is also observed towards the interior of W44, with no clear radio counterpart. We confirm that over most of the source, the bright X-ray emission corresponds with regions of low radio brightness. At the northern border of the remnant, diffuse X-ray emission exactly overlaps the radio and optical radiation. From the study of the immediate environs of W44 we conclude that the remnant is interacting with molecular clouds along the eastern border. Such a scenario is compatible with the filamentary structure of W44, the excitation of OH masers and the apparent lack of optical emission along the eastern border. To the north, an extended atomic cloud surrounds the remnant, although the interaction is not evident in this case. © 1997 American Astronomical Society. [S0004-6256(97)00304-X]

1. INTRODUCTION

Multispectral observations of supernova remnants (SNRs) provide valuable information concerning the physical processes in strong shock waves, as well as the structure of the interstellar medium (ISM) in their vicinity. In the case of composite remnants, their radio emission includes a shell-type component, with a steep non-thermal spectrum, and a central core with a flatter spectrum. The nature of this combined emission is relatively well understood (Weiler & Sramek 1988). However, recent X-ray observations have revealed another type of composite remnant classified on the basis of its edge-brightened radio emission together with centrally-peaked X-ray emission. A general understanding of

these “composite” SNRs that can account for their emission characteristics from radio to X rays is lacking (Rho 1995). W44, with both a steep spectrum radio shell and a flat spectrum pulsar-powered core component, and also a center-filled appearance in the X-ray range, turns out to be the first remnant to be a composite in both definitions. It is therefore an ideal candidate for a multiwavelength study of the interactive-composite remnants.

W44 (G34.7–0.4), located at R.A. (1950)=18^h53^m30^s, DEC (1950)=01°18′ appears in the radio range as a rather distorted shell structure with a significant flattening on the northeast edge. The distance is estimated to be 3 kpc based on H I absorption measurements (Green 1989), with an age of 10⁴ yr calculated based on X-ray observations (Smith *et al.* 1985; Rho *et al.* 1994). Smith *et al.* (1985) suggest that the remnant is in its late adiabatic stage, expanding into a cloudy ISM.

Wolszczan *et al.* (1991) reported the discovery of an as-

¹Member of the Carrera del Investigador Científico of CONICET, Argentina.

²Observer at the Burrell Schmidt telescope of the Warner & Swasey Observatory, Case Western Reserve University, located at Kitt Peak, Arizona.



FIG. 1. (a) The SNR W44 in the light of $H\alpha$ obtained by combining five disregistered frames from the Burrell Schmidt telescope. North is up, and east left in this image, and the field is $40'$ square.

sociated 267 ms pulsar, PSR 1853+01, located inside the W44 shell about 9 arcmin south of the geometric center of the remnant. They derived a characteristic age of about 2×10^4 yr for the pulsar, and a distance to the pulsar of 3.2 kpc based on its dispersion measure.

In this paper we report on new optical images of W44, acquired with the Burrell Schmidt telescope at KPNO, which show for the first time the full extent of the optical emission associated with W44. We also report a new radio image of W44 obtained at 1.4 GHz from existing VLA archive data (Jones *et al.* 1993) in the C and D configurations. From this database we produce an accurate comparison of the W44 structure at radio, optical and X-ray wavelengths based on

subarcminute resolution images. We also explore the correlation with the surrounding ISM making use of infrared (*IRAS*), CO, OH, and H I observations.

1.1 Radio Continuum

In the radio regime W44 has been extensively studied at several frequencies from 330 MHz to 10.7 GHz (Kundu & Velusamy 1972; Velusamy & Kundu 1974; Velusamy 1988; Clark *et al.* 1975; Kassim 1992; Jones *et al.* 1993). Polarization of up to 20% was detected at 28 cm (Kundu & Velusamy 1972). This polarization is unusually high for a shell-type remnant (Reynolds 1988). It is probably a manifestation of the uniformity in the distribution of the magnetic field along the brightest portions of the shell.

The best radio image available to date is that by Jones *et al.* (1993), obtained with the VLA at 1465 MHz with a spatial resolution of $15''$. This high resolution image reveals the presence of several filaments across the remnant and distortions (“dents”) along the eastern border that are explained in terms of expansion into a cloudy interstellar me-

TABLE 1. Filter characteristic and exposure times.

Line	λ_c (Å)	FWHM (Å)	Total exposure (s)
$H\alpha$	6561	26	3000
[S II]	6719	49	3000
Continuum	6845	93	1500



(b)

FIG. 1. (b) Same image as in (a), but with a matched red continuum image subtracted to reveal faint nebulosity more clearly.

dium in which most of the mass is in cool dense state. Jones *et al.* (1993) also report the detection of two sources in the vicinity of PSR 1853+01: a weak radio feature 12'' north of the pulsar and a diamond-shaped nebula 1'.5 north. The authors propose that these radio features are relic synchrotron nebulae left behind by the fast moving pulsar. As shown below, based on the present observations, we can demonstrate that these two discrete sources are indeed part of a single cometary shaped structure, with the pulsar located at the apex. Frail *et al.* (1996a) confirmed the pulsar wind origin for this nebula.

Kassim (1992) estimates the global spectral index α ($S \propto \nu^\alpha$) to be between -0.3 and -0.4 , a value somewhat flatter than the observed in most shell-type radio remnants (typically a mean value of -0.45 , Reynolds 1988). Kovalenko *et al.* (1994), based on a wider spectral range, confirm this result with a spectral index of -0.33 ± 0.05 for W44.

1.2 X-ray and Optical

The first X-ray survey of W44 was carried out using the Einstein IPC by Smith *et al.* (1985), who found it to have a

centrally peaked ("plerionic") X-ray morphology, similar to other SNRs such as 3C400.2, W28, and W49B. Early evidence of line emission indicated that the X-rays have a thermal origin and high absorption, facts which led Smith *et al.* to suggest that W44 might, in fact, be a shell-like Sedov remnant, but that only the high-temperature interior is visible through the absorption column. The discovery of a fast radio pulsar within W44 suggests that part of the X-ray flux might be radiated by "fossil" electrons left over from the pulsar's early life (Wolszcan *et al.* 1991). However, no direct evidence for either a point source or a synchrotron nebula appeared in any X-ray studies until the recent ASCA observation by Harrus *et al.* (1996). They report detection of a hard (≥ 4 keV) X-ray source coincident with PSR 1853+01 and extended over a region between 30'' and 5' in size. The X-ray spectrum from the pulsar region has a nonthermal excess, which Harrus *et al.* interpret as an X-ray synchrotron nebula, the counterpart to the radio nebula studied by Frail *et al.* (1996a) (see Sec. 1.1).

The vast majority of the X-ray flux appears at energies below 4 keV and is of thermal origin. This has recently been

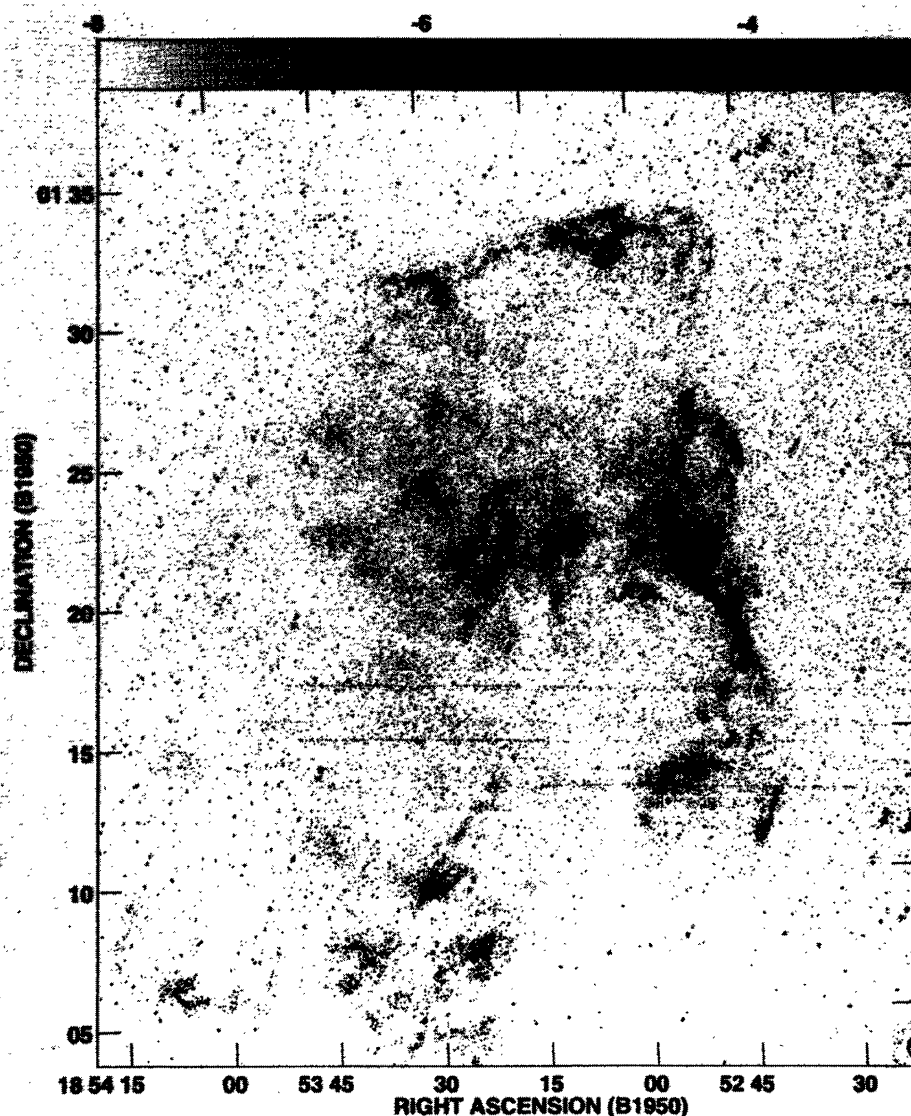


FIG. 2. W44 in the light of [S II], with a scaled continuum image subtracted.

mapped using the *ROSAT* PSPC by Rho *et al.* (1994), who find the same extended, centrally peaked morphology reported by Smith *et al.* (1985) from the Einstein IPC. In an attempt to understand how thermal X rays arise from a morphology so different from a limb-brightened shell, Jones *et al.* (1993) and Rho *et al.* (1994) have carried out independent detailed analyses of X-ray spectra from *EXOSAT*, the Einstein SSS, and (in the case of Rho *et al.*) the *ROSAT* PSPC. Both groups find that the X-ray structure and spectrum can be well explained through an evaporation model first proposed by White & Long (1991): most of the mass of the ISM resides in dense clumps; these gradually evaporate following passage of the supernova shock, to produce a reservoir of hot plasma which radiates thermal X rays.

Rho *et al.* (1994) also present the first images to show optical emission from W44. Their CCD mosaics from the Palomar 1.5 m telescope cover most of the radio shell of W44 and show a coarse filamentary morphology which is

very similar in both $H\alpha$ and [S II] $\lambda\lambda$ 6717, 6731. Rho *et al.* compared their X-ray image with a low angular resolution ($3'$ FWHM) 408 MHz radio map by Clark *et al.* (1975).

1.3 The Surrounding Medium

Several studies have been performed in atomic and molecular lines of interstellar gas in the direction of W44, showing the existence of a complex of clouds near the SNR (e.g., Sato 1986, and references therein). However, no definite conclusions have been reached regarding how the SNR and the clouds are interacting with each other (Venger *et al.* 1981; De Noyer 1983; Sato 1986). A recent investigation by Koo & Heiles (1991, 1995) led to the detection of a high velocity ($v \sim 150 \text{ km s}^{-1}$) H I shell associated with W44, interior to the radio shell. They interpret these observations in terms of a model of W44 exploding inside a wind-blown cavity (the H I structure) that has been rejuvenated and dis-

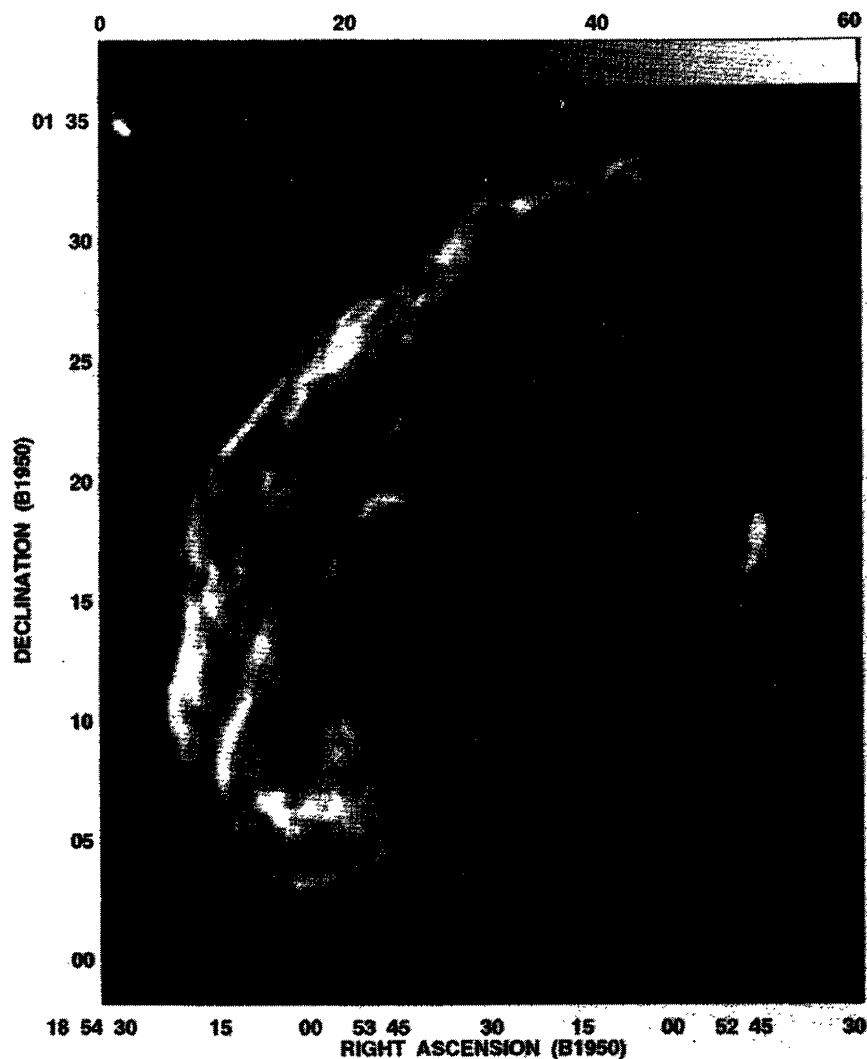


FIG. 3. Greyscale image of the SNR W44 at 1442.5 MHz. The beam is $15''.8 \times 15''.4$. The greyscale range is 10–60 mJy/beam. The cross indicates the position of the pulsar PSR 1853+01 (Frail *et al.* 1996a).

rupted by the supernova blast-wave (the outer radio shell). Maciejewski *et al.* (1996) surveyed in the H I line the region $30^\circ \leq l \leq 40^\circ$, $-15^\circ \leq b \leq -1^\circ$, close to W44 ($21'$ FWHM). Based on these observations, they propose that this SNR lies at the base of a bright H I cone connected with a 5.6 diameter H I shell, the Aquila Supershell. Seta (1996) performed high-resolution CO observations in the direction of W44 using the 45 m NRO telescope, confirming the presence of molecular clouds along the eastern limb of the remnant. In addition, Claussen *et al.* (1996) carried out observations of the 1720 MHz OH maser transition at high angular resolution ($1''$) in W44. They detected two groups of OH masers that they argue may be collisionally excited by the passage of the W44 SNR shock through a molecular cloud.

In the infrared domain, Arendt (1989) reported a number of IR sources around W44, near its northwestern edge; Saken *et al.* (1992), in a survey of IR emission originating in galac-

tic SNRs, concluded that there is no extended IR emission matching the radio remnant.

The present paper is organized as follows in Sec. 2 we present the observations and results. In Sec. 3 we compare the morphology in the different spectral regimes. In Sec. 4 we study the interaction with the surrounding medium and in Sec. 5 we summarize the results.

2. OBSERVATIONS AND RESULTS

2.1 Optical Images

W44 was observed with the 0.6 m Burrell Schmidt telescope at KPNO, together with the S2KA CCD camera, on 1993 June 22–24. Observations were made through interference filters with pass bands centered on H α and [S II] $\lambda\lambda$ 6717, 6731, plus a continuum band which was used for star subtraction. Frames were taken through each filter at five

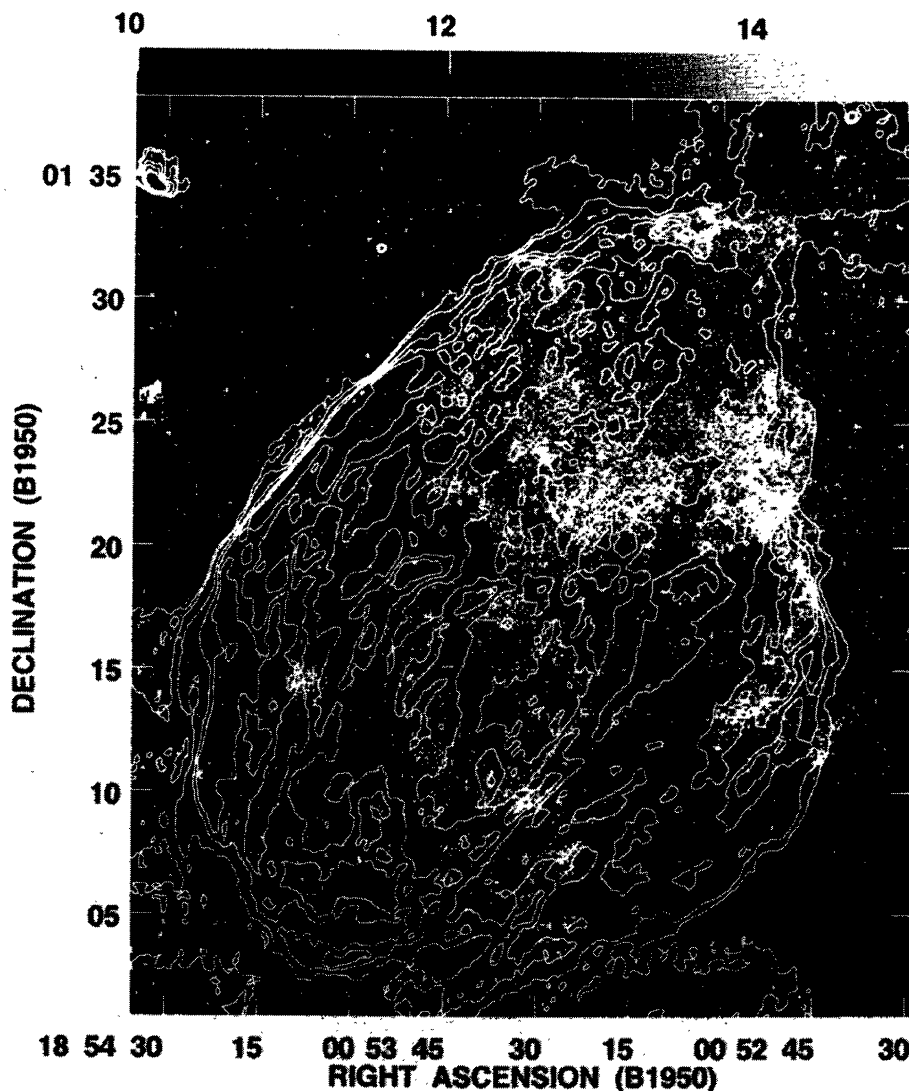


FIG. 4. Greyscale image of the $H\alpha$ emission of W44 with contours of the 1442.5 MHz emission. The radio contours are 10, 15, 25, 35, and 45 mJy/beam.

locations, all centered close to the center of W44, but disregarded to minimize the effects of severe cosmetic blemishes which afflict the S2KA chip. Details of the filters and exposures are given in Table 1. The unvignetted field of the S2KA chip on the Schmidt was almost 1° , easily encompassing W44 in its entirety within the field at each pointing position. The scale of the images is $2.03 \text{ arcsec pixel}^{-1}$, and the resolution, based on the FWHM of stellar images around the field, is about 4 arcsec.

The images have been processed using conventional IRAF techniques: bias subtraction and flat fielding using a combination of several well-exposed twilight sky flats. All the frames were then registered to fractional-pixel accuracy using stars that appear in all the fields and combined, according to the procedures outlined in Winkler *et al.* (1993).

Figure 1(a) shows the $H\alpha$ mosaic image, while Fig. 1(b) shows the same image with the scaled continuum mosaic subtracted to remove most of the stars and reveal faint nebula-

osity. Figure 2 shows the continuum-subtracted $[S \text{ II}]$ image. A high degree of foreground absorption just south of W44 is apparent in all the images, and absorption is probably variable across W44 itself.

The brightest features in the $H\alpha$ image have surface brightness $1.0 \times 10^{-16} \text{ ergs cm}^{-2} \text{ s}^{-1} \text{ arcsec}^{-2}$, while the faintest features visible in the image have surface brightness only $\sim 10^{-17} \text{ ergs cm}^{-2} \text{ s}^{-1} \text{ arcsec}^{-2}$ above the local diffuse background.

2.2 Radio Images

The observations at 1.4 GHz were done with the VLA in the C and D configuration in 1984 and 1985 (Jones *et al.* 1993). The UV data were taken from the VLA archive and reprocessed. Both C-array and D-array UV visibilities were concatenated and combined with single dish data. Data corresponding to the shorter spacings were extracted from Con-

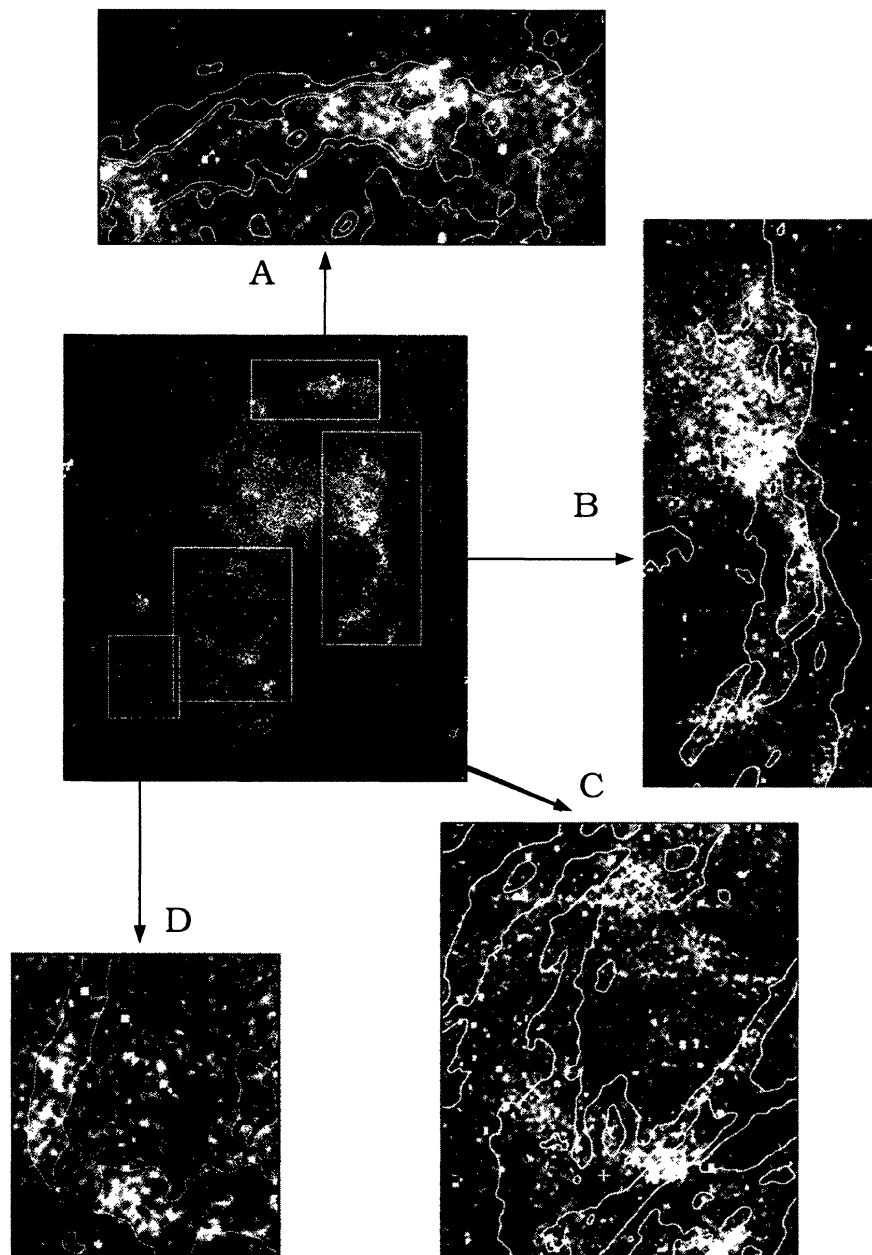


FIG. 5. Enlargements of four areas in the $H\alpha$ image with some radio contours overlapping.

don & Broderick (1985, 1986) 1400 MHz survey ($12'.7 \times 11'.1$ resolution). The interferometric and single dish data were combined through the AIPS task IMERG. In this way the total flux density was recovered, obtaining $S = (210 \pm 20)$ Jy at 1442.5 MHz. The resulting synthesized beam is $15''$ and the noise level is 12 mJy/beam.

Figure 3 displays a greyscale image of W44 at 1442.5 MHz; the cross indicates the new position of PSR 1853+01 (see below). This high-resolution image shows an elongated shell of about $35' \times 24'$ in size, with numerous knots and filamentary arcs of synchrotron radiation, both in the interior and along the perimeter of W44 in good agreement with the image of Jones *et al.* (1993). However, with the addition of

short spacings we are able to show that the two discrete sources seen by Jones *et al.* (1993) (i.e., the “diamond” nebula $1'.5$ north and the extended emission $12''$ north of the pulsar) form a single structure, with the pulsar lying on its southern border. The position of the pulsar PSR 1853+01 was redetermined (Frail *et al.* 1996a) at $18^h53^m38^s.33$, $01^\circ09'26''.1$ with an accuracy of $\sim 1''.5$.

Complementary observations of this SNR were performed with the VLA at 330 MHz in the D configuration (1996 September 3). These observations consisted of a set of snapshot with a total integration time of about one hour. The final image has a flux density of 400 ± 40 Jy, an angular resolution of $\approx 3'$ and an rms noise level of about 140 mJy/beam. The

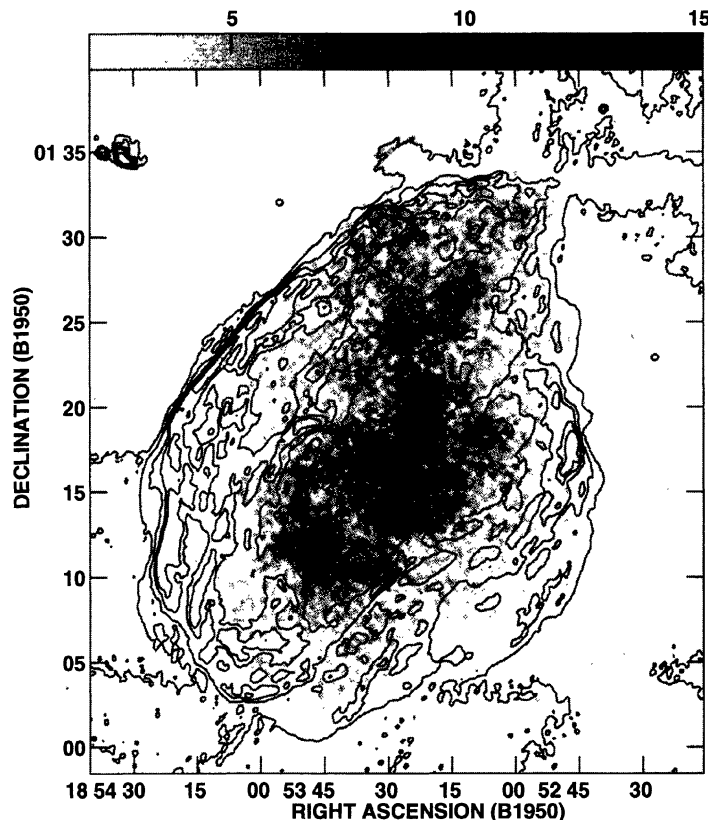


FIG. 6. Overlay of the *ROSAT* X-ray image of W44 as taken from Rho *et al.* (1994) with contours of the 1442.5 MHz emission. The radio contours are 10, 20, 30, 40, and 50 mJy/beam.

330 MHz image of W44 confirms the overall structures as seen in the high-resolution 1442.5 MHz image. Based on the current 0.3 and 1.4 GHz data, we obtained a spectral index $\alpha \approx -0.40$ for the whole remnant, in agreement with the estimates of Kassim (1992) and Kovalenko *et al.* (1994). To investigate the spectral index distribution across W44 we have smoothed the 1442.5 MHz map to the resolution of the 330 MHz map and regridded to the same pixel positions. Taking into account the flux error margins at both frequencies and the background bias, we conclude that the spectral index is roughly constant across the remnant.

3. COMPARISON WITH OPTICAL AND X-RAY EMISSIONS

Figure 4 shows an overlay of radio contours at 1442.5 MHz with the continuum subtracted $H\alpha$ image. The optical emission appears entirely confined within the radio shell. A remarkable correspondence between regions of $H\alpha$ emission and radio emission is observed in different parts of the remnant. As was noted by Rho *et al.* (1994), there is excellent morphological correspondence between the brightest features in the $H\alpha$ image (Fig. 1) and the [S II] image (Fig. 2). [S II] is known to be tracer of hot, shocked gas in regions where expanding SNR shells encounter and overtake density enhancements in the surrounding interstellar medium. The presence of shocked interstellar gas as delineated by our $H\alpha$ and [S II] images indicates the presence of radiative shocks (Draine & McKee 1993). Regions behind radiative shocks

are known to undergo strong compression, therefore, such conditions are expected to result in both an amplification of magnetic fields and enhancements in relativistic particle densities. The excellent correspondence between regions of [S II] and $H\alpha$ emission with regions of enhanced synchrotron emission, as delineated from our continuum image (Fig. 3), confirms this scenario.

The combination of high-resolution radio data and optical image covering the entire remnant reveals some strong radio-optical correlations, as shown in Fig. 5. Region A, to the north of the remnant, shows the brightest optical filaments exactly coincident in location and shape with the radio features. Also a short curved optical filament, partially shown in the lower left corner of region A (see also Fig. 2), has an identical radio counterpart, clearly visible in the grey-scale image in Fig. 3 as the small arc protruding on the northern border. These correspondences were not previously noticed by Rho *et al.* (1994) because their $H\alpha$ image did not cover all of W44. Region B is another example of good agreement between radio and optical emission. As in region A, the optical emission is confined within the shock front defined by the outer radio contour. Both regions (A and B) are also very bright in [S II] (Fig. 2).

Region C displays an area close to the pulsar PSR 1853 +01. In this region the optical emission trace an almost complete circle, with the pulsar located on the southern border. It is only partially correlated with the radio emission, mainly

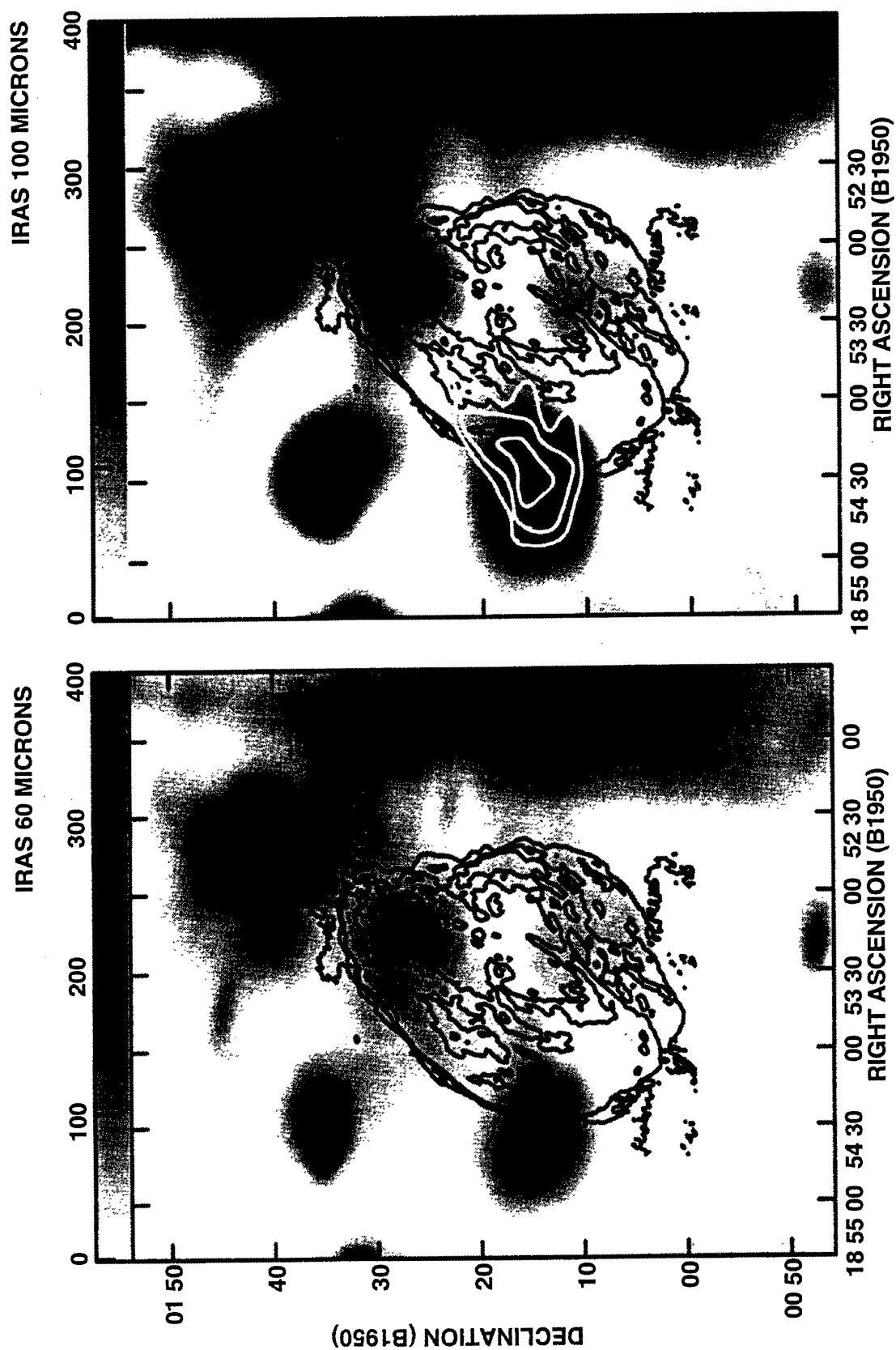


FIG. 7. Comparison of the *IRAS* infrared emission at 60 μm (left) and 100 μm (right) with the radio continuum emission at 1442.5 MHz. The white contours represent the ^{13}CO cloud as taken from Wootten (1977).

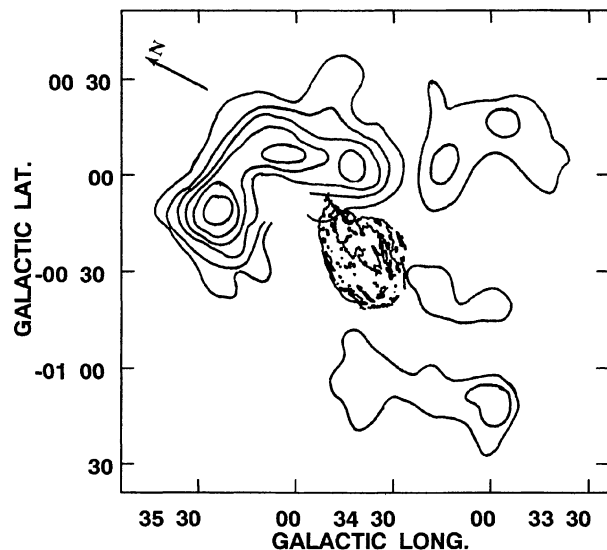


FIG. 8. Contour map of the cold H I optical depth at $v = +45 \text{ km s}^{-1}$ as taken from Sato (1986), together with contours of the 1442.5 MHz emission. The plotted contours correspond to $\tau(\text{H I}) = 0.1, 0.15, 0.2, 0.25, 0.3$, and 0.35 .

along the southwestern part of the H α ring. Region D shows another faint optical ring-like feature, in this case very well correlated with the radio emission.

No radio counterpart is evident for the rest of the optical remnant (the diffuse optical emission observed near $18^{\text{h}}53^{\text{m}}30^{\text{s}}, 01^{\circ}22'$ in Fig. 4). This lack of correlation suggests that a different physical process may give rise to the H α emission in this case. As seen in Fig. 2, this nebulosity appears fainter in the [S II] line than towards the north and northwestern shocked filaments.

Figure 6 shows contours of 1442.5 MHz radio emission superposed on a greyscale representation of the *ROSAT* X-ray emission as taken from Rho *et al.* (1994). As noticed by Rho *et al.* (1994) the brightest soft X-ray emission is concentrated towards the center of the remnant, where it has a knotty and irregular distribution. No special correspondence is found between the X-ray maxima and radio continuum features. A previously unnoticed fact is that the diffuse X-ray emission extends beyond the central region up to the north where it perfectly matches the radio and optical border.

4. W44 AND THE SURROUNDING MEDIUM

As summarized in Sec. 1.3, several atomic and molecular line studies have been performed in the direction of W44. From the comparison of the present high-resolution radio images with available observations, we can constrain the geometry of the area where W44 evolves and investigate the impact of the remnant on the surrounding interstellar clouds.

Figure 7 shows the infrared emission around W44 as shown by *IRAS* images at $\lambda 60 \mu\text{m}$ and $100 \mu\text{m}$ with overlapping contours of the radio continuum emission. The emission at $100 \mu\text{m}$ is brighter than at $60 \mu\text{m}$, a spectral trend

compatible with a shock heated dust origin (Junkes *et al.* 1992). The thick white contours near $18^{\text{h}}54^{\text{m}}30^{\text{s}}, 01^{\circ}15'$, shown in the image at $100 \mu\text{m}$, reproduce the 45 km s^{-1} ^{13}CO cloud reported by Wootten (1977) to be at a kinematical distance compatible with the distance of 3 kpc estimated for W44 (Green 1989). Excellent correlation is found between infrared and molecular emission over the eastern cloud. Faint IR emission is also observed towards the north and in the interior of W44 near $18^{\text{h}}53^{\text{m}}17^{\text{s}}, 01^{\circ}27'30''$, and $18^{\text{h}}53^{\text{m}}22^{\text{s}}, 01^{\circ}11'15''$, respectively. The bright IR feature observed to the west of W44 was previously reported by Arendt (1989) as possibly related to W44. Based on the present comparison, the location of the IR feature is too far from the borders of the remnant to infer a physical association with W44.

Seta (1996)'s millimeter observations confirm the presence of the ^{13}CO cloud observed by Wootten (1977), partially overlapping the southeastern border of W44. From the images obtained by Seta (1996) an additional CO feature, ($v \sim 43 \text{ km s}^{-1}$) is observed near $18^{\text{h}}53^{\text{m}}52^{\text{s}}, 01^{\circ}28'$. This last cloud appears elongated in shape, approximately $4.5 \times 9'$ in size is adjacent to the highly compressed northeast border, where several bright radio filaments are observed. The CO cloud lies slightly to the north of two of the groups of 1720 OH masers reported by Claussen *et al.* (1996) located near $18^{\text{h}}53^{\text{m}}56.8^{\text{s}}, 01^{\circ}25'11''$ and $18^{\text{h}}54^{\text{m}}04.5^{\text{s}}, 01^{\circ}22'34''$. These masers are thought to be collisionally excited by H_2 molecules following the passage of a shock through the molecular gas (Frail *et al.* 1996b, and references therein), and thus are independent evidence that W44 is undergoing an interaction with a molecular cloud along its eastern edge.

We also examined all the previous studies of H I carried out in the vicinity of W44. In Fig. 8, we show the spatial correlation between our radio image and the contour image of the cold H I optical depth at the absorption maximum near $v \sim +45 \text{ km s}^{-1}$ as obtained by Sato (1986) (12.5 FWHM). As far as we know, this is the only study of H I available that enables to produce a global picture of the cold gas distribution around W44, because the observations are performed in a large angular field around the remnant and cover a velocity range compatible with its distance. With the improvement in the angular resolution of the present radio image we can confirm Sato's suggestion, that the SNR may not be "making contact" in the plane of the sky with the northern cold H I cloud. To the south, the presence of an absorbing cold cloud near $l \sim 34^{\circ}30', b \sim -0^{\circ}30'$, can explain the apparent lack of optical emission that can be noticed in the lower right corner in Fig 4. New H I observations, performed in a wide field around W44 with higher angular resolution and sensitivity may help to investigate the physical interaction of the cold gas with W44.

5. SUMMARY

In this paper we have examined the SNR W44 and produced accurate multispectral comparisons. VLA archive data acquired in 1984 and 1985 for W44 at 1.4 GHz in the C and D configurations were reprocessed adding the short spacing

contribution from single dish observations, in order to obtain an image sensitive to structures larger than 15 arcmin. The subsequent image emphasizes the filamentary structure of the remnant, as well as the presence of diffuse emission in the interior. VLA data obtained at 330 MHz in the D configuration resulted in an image of similar morphology, with no evidence for significant spectral index variations across the source. From the 330 and 1442.5 MHz data we derived a constant spectral index $\alpha \approx -0.4$ for this supernova remnant in agreement with previous estimates.

We obtained new optical images in the H α and [S II] lines by mosaicing the full extent of the remnant. The optical emission is in general diffuse, brighter in the upper half of the remnant and with a ring-like feature, centered near 18^h53^m40^s, 01°14', projected onto the interior of W44 with the pulsar on its southern border. These new optical images were compared with the radio emission at 1.4 GHz. The correlation is very good, mainly towards the north and north-western sides, where the optical emission appears to be precisely correlated with the radio emission. The correlation of the optical emission with bright synchrotron emission is consistent with the presence of enhanced magnetic fields and high relativistic particles densities expected in the compressed regions associated with radiative shock processes. This suggests that the optical emission arises from shocked, radiatively cooling gas.

We also compared the radio continuum images with the soft *ROSAT* X-ray image. In general we confirm the conclusions of Rho *et al.* (1994), suggesting that X-ray emission appears centrally concentrated, surrounded by a thick radio shell. However, based on the present images, we have shown that weaker diffuse X-ray emission extends up to the northern radio boundary of W44.

By comparing our new images with IR and atomic and molecular lines studies, we have explored the mutual interaction of W44 with its inhomogeneous surroundings. Based on the radio and CO comparisons we can speculate that the SN shock along the east side is physically interacting with the CO clouds reported by Wooten (1977) and Seta (1996). The molecular clouds overlap part of the front face of W44.

Such a geometry provides a plausible explanation not only for the lack of optical emission in the east, since it would be obscured by the clouds, but also for the presence of the shock excited OH masers observed projected against the eastern border of W44, and for the IR emission observed with spectral characteristics compatible with shock heated dust. The existence of IR emission in a site where different evidences suggest a physical interaction between the SN shock wave and the molecular cloud, may be a promising indicator of a location to conduct a search for protostellar candidates within the cloud, and investigate star formation triggered by a SN explosion.

From the comparison of our radio image with the available observations of the H I in the direction of W44, we do not see clear evidence of a direct interaction between the SN shock and the cold neutral interstellar gas which surrounds W44. High spatial resolution observations of H I around W44 would be very helpful in order to provide a good diagnostic of the interaction with the surrounding cold gas.

From the available observational data, we can infer that at large scales, the interaction with surrounding molecular clouds have substantially contributed to the formation of the present filamentary morphology of W44 as seen in radio wavelengths.

E.G. and G.D. acknowledge the support received from NRAO during their stay at the VLA. This research was part of a Cooperative Science Program between NSF (USA) and CONICET (Argentina). The National Radio Astronomy Observatory (NRAO) is a facility of the National Science Foundation operated under a cooperative agreement by Associated Universities, Inc. This research had made use of data obtained from the US *ROSAT* Public Data Archive which is jointly managed by the *ROSAT* Science Data Center and the HEASARC. PFW and BFW acknowledge the support of the NSF throughout Grant No. AST-9315967 and of the W. M. Keck Foundation through the Keck Northeast Astronomy Consortium. Basic research in radio astronomy at the Naval Research Laboratory is supported by the Office of Naval Research.

REFERENCES

- Arendt, R. G. 1989, *ApJS*, 70, 181
 Clark, D. H., Green, A. J., & Caswell, J. L. 1975, *AuJPA*, 37, 75
 Claussen, M. J., Frail, D. A., Goss, W. M., & Gaume, R. A. 1996, in preparation
 Condon, J. J., & Broderick, J. J. 1985, *AJ*, 90, 2540
 Condon, J. J., & Broderick, J. J. 1986, *AJ*, 91, 1051
 De Noyer, L. K. 1983, *ApJ*, 264, 141
 Draine, B. T., & McKee, C. F. 1993, *ARA&A*, 31, 373
 Frail, D., Giacani, E. B., Goss, W. M., & Dubner, G. M. 1996a, *ApJ*, 464, L165
 Frail, D. A., Goss, W. M., Reynoso, E. M., Giacani, E. B., Green, A. J., & Otrupcek, R. 1996b, *AJ*, 111, 1651
 Green, D. A. 1989, *MNRAS*, 238, 737
 Harrus, I. M., Hughes, J. P., & Helfand, D. J. 1996, *ApJ*, 464, L161
 Jones, L. R., Smith, A., & Angellini, L. 1993, *MNRAS*, 265, 631
 Junkes, N., Fürst, E., & Reich, W. 1992, *A&A*, 261, 289
 Kassim, N. 1992, *AJ*, 103, 943
 Koo, B.-C., & Heiles, C. 1991, *ApJ*, 382, 204
 Koo, B.-C., & Heiles, C. 1995, *ApJ*, 442, 679; Kovalenko, A. V., Piznar, A. V., & Udal'tsov, V. A. 1994, *Astron. Rep.* 38, 78
 Kovalenko, A. V., Piznar, A. V., & Udal'tsov, V. A. 1994, *Astro. Rep.*, 38, 78
 Kundu, M. R., & Velusamy, T. 1972, *A&A*, 20, 237
 Maciejewski, W., Murphy, E. M., Lockman, F. J., & Savage, B. D. 1996, *ApJ*, (in press)
 Reynolds, S. P. 1988, in *Galactic and Extragalactic Radio Astronomy*, edited by G. L. Verschuur and K. L. Kellerman (Springer, New York), p. 439
 Rho, J. H. 1995, Ph.D. thesis, University of Maryland
 Rho, J. H., Petre, R., Schlegel, E. M., & Hester, J. 1994, *ApJ*, 430, 757
 Saken, J. M., Fesen, R. A., & Shull, J. M. 1992, *ApJS*, 81, 715
 Sato, F. 1986, *AJ*, 91, 378
 Seta, M. 1996, Ph.D. thesis, University of Tokyo
 Smith, A., Jones, L. R., Watson, M. G., & Willingate, R. 1985, *MNRAS*, 217, 99
 Velusamy, T. 1988, in *Supernova Remnants and the Interstellar Medium*,

- Proceedings of IAU Colloquium N° 101, edited by R. S. Roger and T. L. Landecker (Cambridge University Press, Cambridge), p. 266
- Velusamy, T., & Kundu, M. R. 1974, *A&A*, 32, 375
- Venger, A. P., Gosachinskii, I. V., Grachev, V. G., Egorova, T. M., Ryzhkov, N. F., & Khersonskii, V. K. 1981, *SvA*, 25, 675
- Weiler, K. W., & Sramek, R. A. 1988, *ARA&A*, 26, 295
- White, R. L., & Long, K. S. 1991, *ApJ*, 373, 543
- Winkler, P. F., Olinger, T. M., & Westerbeke, S. A. 1993, *ApJ*, 405, 608
- Wolszczan, A., Cordes, J. M., & Dewey, R. J. 1991, *ApJ*, 372, L102
- Wootten, H. A. 1977, *ApJ*, 216, 440